

Unified framework for Early Dark Energy from α -attractors

Matteo Braglia,^{1,2,3,*} William T. Emond,^{4,†} Fabio Finelli,^{2,3,‡} A. Emir Gümrükçüoğlu,^{5,§} and Kazuya Koyama^{5,¶}

¹*Dipartimento di Fisica e Astronomia, Alma Mater Studiorum Università di Bologna,
Via Gobetti, 93/2, I-40129 Bologna, Italy*

²*INAF/OAS Bologna, via Gobetti 101, I-40129 Bologna, Italy*

³*INFN, Sezione di Bologna, Via Bertini 6/2, I-40127 Bologna, Italy*

⁴*School of Physics and Astronomy, University of Nottingham,
University Park, Nottingham NG7 2 RD, United Kingdom*

⁵*Institute of Cosmology and Gravitation, University of Portsmouth,
Dennis Sciama Building, Portsmouth PO1 3FX, United Kingdom*

(Dated: August 31, 2022)

One of the most appealing approaches to ease the Hubble tension is the inclusion of an early dark energy (EDE) component that adds energy to the Universe in a narrow redshift window around the time of recombination and dilutes faster than radiation afterwards. In this paper, we analyze EDE in the framework of α -attractor models. As well known, the success in alleviating the Hubble tension crucially depends on the shape of the energy injection. We show how different types of energy injections can be easily obtained, thanks to the freedom in choosing the functional form of the potential inspired by α -attractor models. To confirm our intuition we perform an MCMC analysis for three representative cases and find indeed that H_0 is significantly larger than in Λ CDM like in other EDE models. Unlike axion-driven EDE models with super Planckian decay constant, the curvature of EDE models required by the data is natural in the context of recent theoretical developments in α -attractors.

I. INTRODUCTION

Recent low-redshifts distance-ladder measurements suggest a larger Hubble constant H_0 than the one determined from cosmic microwave background (CMB) data [1]. The value of H_0 inferred from the latest *Planck* 2018 data, $H_0 = (67.36 \pm 0.54) \text{ km s}^{-1} \text{ Mpc}^{-1}$ [2], is in a 4.4σ tension with the most recent distance-ladder measurement from the SH0ES team [3], $H_0 = (74.03 \pm 1.42) \text{ km s}^{-1} \text{ Mpc}^{-1}$ which is determined by using type Ia supernovae (SNe Ia) as standard candles [4]. Other low-redshift methods to determine H_0 , such as from strong-lensing time delay [5] or from calibrating SNe Ia by the tip of the red giant branch [6–8], also point to a higher H_0 than in Λ CDM. In absence of unknown systematics, new physics seems necessary to solve this H_0 tension [9].

A common approach to model building consists of increasing the expansion rate at redshifts around matter-radiation equality in order to shrink the comoving sound horizon at baryon drag r_s , which results in a higher H_0 inferred from CMB [10, 11]. The addition of light relics is a typical example that helps ease the tension by changing the early-time dynamics of the Universe [12–16]. Modified gravity models also lead to interesting solutions to the H_0 tension [17–25].

However, given the success of the Λ Cold Dark Matter (Λ CDM) concordance model in fitting CMB anisotropies,

the early time deviation from it must be minimal. To this end, the Early Dark Energy (EDE) scenario is perhaps the most minimal modification to the Λ CDM background dynamics that substantially alleviates the H_0 tension. In this model, first proposed in [26], a very light scalar field ϕ is frozen by Hubble friction during radiation era, acting as DE with an equation of state $w_{\text{EDE}} \equiv P_{\text{EDE}}/\rho_{\text{EDE}} = -1$ and contributing negligibly to the energy budget of the Universe. Eventually, when the Hubble rate becomes smaller than its effective mass $\partial^2 V(\phi)/\partial \phi^2$, the scalar field quickly rolls down its potential and oscillates around its minimum, its energy diluting faster than radiation. This results in a very sharp energy injection to the cosmic fluid, that for a suitable value of the mass of ϕ occurs around matter-radiation equivalence, successfully lowering r_s . Since the seminal work in [26], a substantial effort has been made in building new models of EDE [27–34] and testing their predictions against larger datasets [35, 36].

In this work, we consider EDE in the framework of α -attractors [37–39], in which the potential for the EDE scalar field is given by

$$V(\phi) = f^2 \left[\tanh(\phi/\sqrt{6\alpha}M_{\text{Pl}}) \right]. \quad (1)$$

This potential arises naturally by turning a non-canonical kinetic pole-like term of the form $[\alpha/(1 - \varphi^2/6M_{\text{Pl}}^2)](\partial\varphi)^2/2$ into a canonical one. Through the field redefinition $\phi = \sqrt{6\alpha}M_{\text{Pl}} \tanh^{-1}(\varphi/\sqrt{6}M_{\text{Pl}})$, the kinetic term becomes canonical and the potential acquires the $\tanh(\phi/\sqrt{\alpha}M_{\text{Pl}})$ dependence. Due to this field redefinition, the potential flattens to a plateau at large values of ϕ . α -attractor models were first introduced in the context of inflation, with predictions for the spectral index n_s and tensor-to-scalar ratio r , largely independent

* matteo.braglia2@unibo.it

† william.emond@nottingham.ac.uk

‡ fabio.finelli@inaf.it

§ emir.gumrukcuoglu@port.ac.uk

¶ kazuya.koyama@port.ac.uk

on the specific functional form of $V(\phi)$, hence the name “attractors”. In the context of dark energy, α -attractor models with an energy scale far below the one used in inflation were considered in [40, 41]. An interesting connection between dark energy and inflation for α -attractor models has also been investigated in [42, 43].

In our EDE proposal, however, the shape of the potential away from the plateau and around its minimum is crucial, as it regulates the shape of the energy injection. One of the *attractive* features of α -attractor models with the potential in Eq. (1), is that they can easily accommodate various types of energy injection. Indeed, we will show that, depending on the functional form of $V(\phi)$, a smooth or oscillating energy injection can be produced, reproducing results of all earlier works in the field in a single framework [26, 27, 29].

This paper is organized as follows. In Sec. II, we describe the background evolution of the model and compare it to existing EDE models, focusing on the shape of the energy injection. We confirm the capability of our model to alleviate the H_0 tension by performing an MCMC analysis in Sec. III and comment on our results in Sec. IV. We end in the conclusions V.

II. BACKGROUND EVOLUTION AND ENERGY INJECTION

Our model is described by the following Lagrangian

$$\mathcal{L} = \sqrt{-g} \left[\frac{M_{\text{pl}}^2}{2} R - \frac{(\partial\phi)^2}{2} - V(\phi) \right] + \mathcal{L}_m, \quad (2)$$

where \mathcal{L}_m is the Lagrangian for matter (including baryons, CDM, photons and neutrinos) and the potential is:

$$V(\phi) = \Lambda + V_0 \frac{(1 + \beta)^{2n} \tanh(\phi/\sqrt{6\alpha}M_{\text{pl}})^{2p}}{[1 + \beta \tanh(\phi/\sqrt{6\alpha}M_{\text{pl}})]^{2n}}, \quad (3)$$

where V_0 , p , n , α and β are constants. The potential corresponds to the simple form $V(\varphi) = \Lambda + \tilde{V}_0 x^{2p}/(1 + \tilde{\beta} x^{2n})$ for the field φ with a pole-like kinetic term and has an offset with respect to Ref. [40, 41]¹, which is admitted in the dark-energy context with α -attractors [43]. We have inserted the normalization factor of $(1 + \beta)^{2n}$ to ensure the same normalization of the plateau at large $\phi > 0$ for every choice of (p, n) . For simplicity we will consider $\beta = 1$ in the following and we will use a rescaled scalar field $\Theta \equiv \phi/(\sqrt{6\alpha}M_{\text{pl}})$ when useful.

We show the potential for three particular choices of $(p, n) = \{(2, 0), (2, 4), (4, 2)\}$, that we label **{A, B, C}**

respectively, in Fig 1. The reason for this choice will be clear in the following. Note that the potential is asymmetric around the origin in the last two cases for which $n \neq 0$. As we will see, the potential in Eq. (3) captures all the interesting phenomenological EDE models, but other functional forms can in principle be chosen according to Eq. (1).

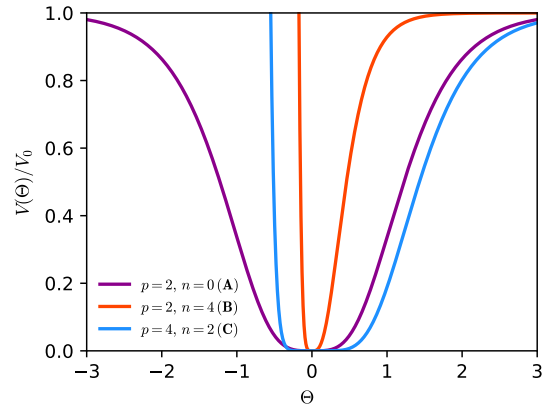


FIG. 1. We plot the potential in Eq. (3) for $(p, n) = \{(2, 0), (2, 4), (4, 2)\}$.

We now discuss the cosmological evolution of α -attractor EDE. The dynamics of the scalar field is similar to other models of EDE studied in the literature and is essentially that of an ultralight axion field [44]. The scalar field starts from its initial value Θ_i deep in the radiation era and remains frozen because of the Hubble friction. The energy density of the scalar field is subdominant in this regime and its equation of state $w_{\text{EDE}} \equiv P_{\text{EDE}}/\rho_{\text{EDE}}$ is equal to -1 , hence the name “Early Dark Energy”. Eventually, the effective mass of the scalar field becomes comparable to the Hubble rate H and ϕ starts to thaw. The redshift z_c at which this occurs can be implicitly defined from the relation $\frac{\partial^2 V(\phi_i)}{\partial \phi^2} \simeq 9H^2(z_c)$ [44]. After z_c , the Hubble friction is too weak to keep the scalar field up its potential and it rolls down in a very short time. When this happens, the potential energy of the scalar field is converted into kinetic one and a certain amount of energy, parameterized by $f_{\text{EDE}} \equiv \rho_{\text{EDE}}(z_c)/3M_{\text{pl}}^2 H^2(z_c)$ is injected to the cosmic fluid. Depending on the slope of the potential and its structure around the minimum, the scalar field then starts to oscillate or simply freezes again once it has exhausted its inertia. The critical redshift z_c and the value of the energy injection f_{EDE} are the key parameters describing all EDE models [45]. As we are going to discuss, the shape of the energy injection and w_{EDE} crucially depend on the different possible dynamics of the scalar field after z_c . The scalar field energy density quickly redshifts away after z_c and its contribution becomes subdominant with respect to the other components of the Universe.

We show in Fig. 2 the EDE dynamics for the three **(A, B and C)** cases mentioned above. In particular, we

¹ Note that in our setting the field rolls towards the minimum of the potential in $\phi = 0$ and not towards infinity as in [40, 41].

plot the scalar field evolution, its equation of state and

the energy injection in the left, central and right panel respectively (see the caption for the parameters used).

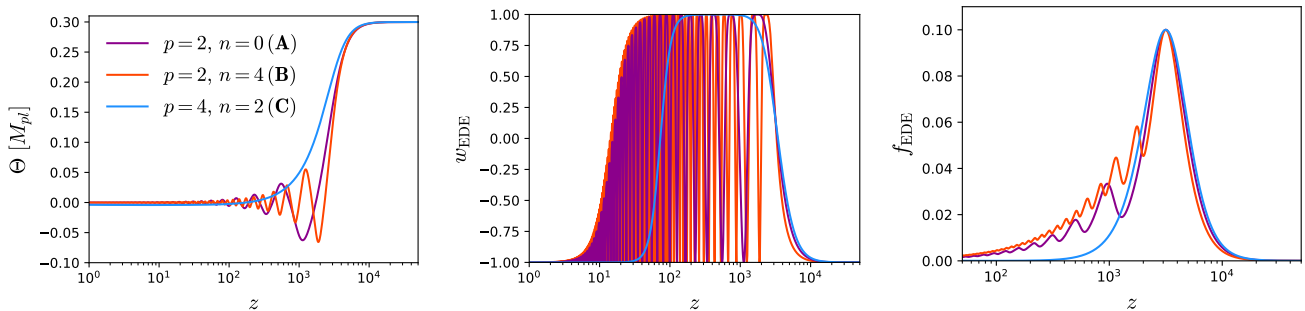


FIG. 2. We plot the evolution of the normalized scalar field Θ [Left], equation of state parameter w_{EDE} [Center] and the energy injection f_{EDE} [Right] for the three models with $(p, n) = \{(2, 0), (2, 4), (4, 2)\}$. For definiteness, we have chosen $f_{\text{EDE}} = 0.1$, $\log_{10} z_c = 3.5$ and $\Theta_i = 0.4$.

In the cases **A** and **B**, the scalar field oscillates at the bottom of its potential leading to a highly oscillatory equation of state. In the **A** case, the potential is $\tanh^4 \Theta \sim \Theta^4$ around $\Theta \simeq 0$ and therefore the shape for the energy injection closely resembles the one obtained in the Rock'n'roll model of Ref. [27] where $V(\phi) \propto \phi^4$. On the other hand, the **B** case looks more similar to the original EDE proposal of Ref. [26] (see e.g. Fig. 2 of Ref. [30]). However, given the asymmetry of our potential for the **B** case, the oscillatory pattern in the energy injection shows an asymmetric amplitude of odd and even peaks in the oscillations. Although this is barely visible in Fig. 2, this effect is more pronounced for larger Θ_i and might in principle lead to distinct results, as the CMB power spectrum is very sensible to the shape of $f_{\text{EDE}}(z)$ [9].

The case **C** is instead different. Unlike the first two oscillatory models, for this choice of p and n , the bottom of the potential is very close to flat and the scalar field shows no oscillations. As anticipated, this model looks indeed similar to the canonical Acoustic Dark Energy (cADE) model proposed in Ref. [29]. As in cADE (see also Ref. [28]), the potential energy is suddenly converted to kinetic one and the scalar field remains in a *kination* regime in which $w_{\text{EDE}} = 1$, and its energy is kinetically dominated until it redshifts away. However, differently from cADE, where the potential was introduced by patching a quartic potential for positive values of ϕ , to $V(\phi) = 0$ for negative ones, our potential **C** arises naturally from the α -attractors construction.

Although we have focused on these three specific cases that well reproduce some cases in the literature, we stress that other possibilities can be obtained for other combinations of the potential parameters (p, n) .

III. COSMOLOGICAL CONSTRAINTS AND IMPLICATIONS FOR THE H_0 TENSION

In this Section, we perform a Markov-Chain Monte Carlo (MCMC) analysis with cosmological data and investigate the capability of α -attractor EDE models to ease the H_0 tension. We use the publicly available code `MontePython-v3`² [46, 47] interfaced with our modified version of `CLASS`³ [48, 49].

We include several datasets in our analysis. We consider CMB measurements from the *Planck* 2018 legacy release (P18) on temperature, polarization, and weak lensing CMB angular power spectra [50, 51]. The high-multipoles likelihood $\ell \geq 30$ is based on `Planck` likelihood. We use the low- ℓ likelihood combination at $2 \leq \ell < 30$: temperature-only `Commander` likelihood plus the `SimAll` EE-only likelihood. For the *Planck* CMB lensing likelihood, we consider the conservative multipoles range, i.e. $8 \leq \ell \leq 400$. To provide late-time information, complementary to the CMB anisotropies, we use the Baryon Spectroscopic Survey (BOSS) DR12 [52] “consensus” results on baryon acoustic oscillations (BAO) in three redshift slices with effective redshifts $z_{\text{eff}} = 0.38, 0.51, 0.61$ [53–55]. Additionally, we use the Pantheon supernovae dataset [56], which includes measurements of the luminosity distances of 1048 SNe Ia in the redshift range $0.01 < z < 2.3$. Finally, we make use of a Gaussian prior based on the determination of the Hubble constant from Hubble Space Telescope (HST) observations, i.e. $H_0 = 74.03 \pm 1.42$ [3].

We study the cosmological models denoted by **A**, **B** and **C** introduced in the previous section. We sample the cosmological parameters $\{\omega_b, \omega_{\text{cdm}}, \theta_s, \ln 10^{10} A_s, n_s, \tau_{\text{reio}}, f_{\text{EDE}}, \log_{10} z_c, \Theta_i\}$ using Metropolis-Hastings algorithm. We consider

² https://github.com/brinckmann/montepython_public

³ https://github.com/lesgourg/class_public

the following flat priors on the EDE parameters: $f_{\text{EDE}} \in [10^{-4}, 0.4]$, $\log_{10} z_c \in [2.9, 4.2]$ and $\Theta_i \in [0.05, 1.4]$. We consider the chains to be converged using the Gelman-Rubin criterion $R - 1 < 0.01$ and adopt the Planck convention modeling free-streaming neutrinos as two massless species and one massive with $M_\nu = 0.06$ eV.

Concerning the linearized perturbations, we impose adiabatic initial conditions and solve the exact evolu-

tion of the scalar field perturbations $\delta\phi(k, \tau)$ in the synchronous gauge [57].

Our results are summarized in Table I, where we report the reconstructed mean values and the 68% and 95% CL, and Fig. 3, which has been obtained using `GetDist`⁴ [58], where we plot the reconstructed two-dimensional posterior distributions of the main and derived parameters. We also plot in Fig. 4 the one-dimensional posterior distributions on the parameters of the potential V_0 and α .

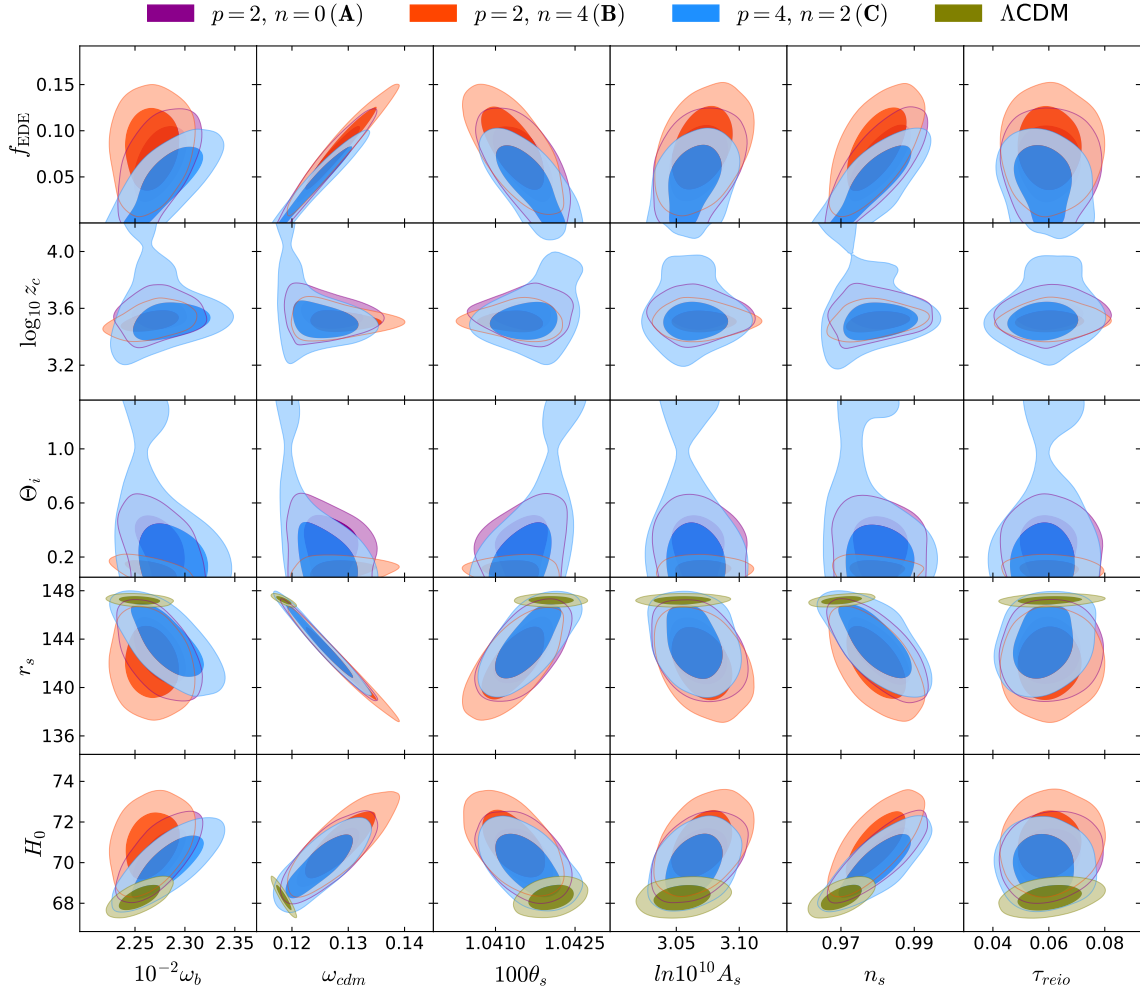


FIG. 3. Constraints on main parameters and H_0 of the α -attractor models **A**, **B** and **C** from Planck 2018 data (P18), BAO, Pantheon and SH0ES data. Parameters on the bottom axis are the standard cosmological parameters, and parameters on the left axis are the EDE parameters that we sample with flat priors, r_s in [Mpc] and H_0 in [$\text{km s}^{-1}\text{Mpc}^{-1}$]. Constraints for the ΛCDM model obtained with the same dataset are also shown. Contours contain 68% and 95% of the probability.

IV. RESULTS

We now comment the results of the previous Section. As expected, all the three cases lead to larger values for the Hubble parameter H_0 , as can be seen from Tab. I. We find that the larger energy injection is allowed in the

model **B** for which $f_{\text{EDE}} = 0.082 \pm 0.029$ results in $H_0 = (70.9 \pm 1.1) \text{ km s}^{-1}\text{Mpc}^{-1}$ at 68% CL. This is followed by model **A** for which $f_{\text{EDE}} = 0.065 \pm 0.026$ results in $H_0 = (70.28 \pm 0.94) \text{ km s}^{-1}\text{Mpc}^{-1}$ and model **C** for which $f_{\text{EDE}} = 0.048^{+0.029}_{-0.024}$ results in $H_0 = (69.88 \pm 0.99) \text{ km s}^{-1}\text{Mpc}^{-1}$.

In all the three models considered, cosmological data require that the initial value for $\Theta_i \sim \mathcal{O}(1)$ after nucleosynthesis, once the slow-roll regime is considered. These values are typical also for other EDE models. For these

⁴ <https://getdist.readthedocs.io/en/latest>

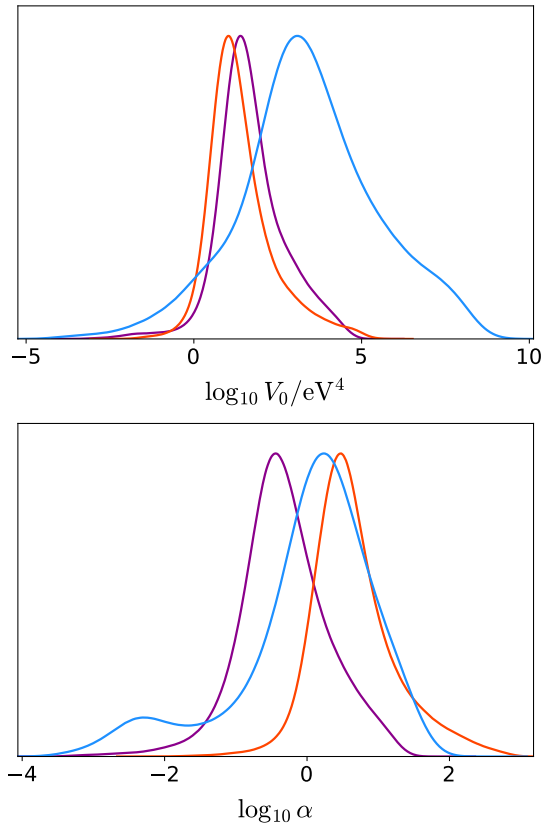


FIG. 4. One dimensional derived posterior distribution of the potential parameters $\log_{10} V_0/\text{eV}^4$ and $\log_{10} \alpha$. The convention for the colors used is the same of Fig. 3.

values, the scalar field is hung up in the descending slope of the potential shown in Fig. 1 after nucleosynthesis: this range of values does not exclude that the scalar field could have been in the plateau outside the slow-roll regime at the beginning of the relativistic era.

Our results are in agreement with the comparison between **A**, **B** and **C** and models in the literature made in the previous Section. Indeed, the higher value of H_0 in the literature of EDE models can be found in the original EDE proposal of Ref. [26]. However, due to our use of more recent CMB data and perhaps the slightly asymmetric oscillations in the energy injection, our inferred value for H_0 is somewhat lower. In fact Ref. [35] also found a H_0 similar to ours when analyzing the model of Ref. [26], adopting the same dataset used here.

Furthermore, contrary to Refs. [27, 29], the potential in Eq. (3) contains two free parameters, and despite the similar shape of the energy injection in the models **A** and **C** respectively, the enhanced number of degeneracies between parameters leads to a slightly different inferred H_0 also in this case.

We note an interesting difference between these EDE models based on α -attractor-like potentials and those inspired by ultralight axionlike fields as Refs. [26, 30, 45]. In models involving cosine potentials, the axion decay

constant f has to take values of order $\mathcal{O}(M_{\text{pl}})$ to solve the H_0 tension [35], in contrast with the weak gravity conjecture [59]. Our results show instead that the allowed range for α is natural in terms of model building and also includes the discrete values for α motivated by maximal supersymmetry [60, 61]. It is also interesting to note that we have here a non-zero detection of α for EDE, whereas at present we have only upper bound on α for inflationary models [62].

V. CONCLUSIONS

In this paper we have studied a new model of Early Dark Energy (EDE) consisting of a minimally coupled scalar field in the framework of α -attractors. As is typical in EDE models, the scalar field remains frozen during radiation era, until it becomes massive and quickly rolls down the potential, injecting a sharp amount of energy to the cosmic fluid and temporarily enhancing the expansion rate of the Universe. The shape of the energy injection is crucial to solve the H_0 tension and depends on the structure of the potential around its minimum. The only constraint in α -attractors is that the potential has to be of the form $V(\phi) = f^2 [\tanh(\phi/\sqrt{\alpha})]$, giving in principle a large freedom to the model building.

Adopting the simple potential in Eq. (3) as a working example, we have shown that it is indeed possible for the energy injection to take several different shapes in the single unified framework of α -attractors and reproduce results from different studies in the literature. To illustrate this, we have analyzed three example models. In the first two (**A** and **B**) the scalar field oscillates at the bottom of the potential in a way that resembles the works [27] and [26] respectively. Note however, that our second example slightly differs from [26] since the asymmetry of the potential around $\phi = 0$ leads to an asymmetric pattern of oscillations in the energy injection. In our third model (**C**), instead, the scalar field never oscillates and quickly transfers its potential energy to kinetic one, undergoing a temporary phase of kination, as in Ref. [29].

We have used the latest *Planck* 2018 CMB temperature, lensing and polarization data together with a variety of high and low z BAO measurements, SNe Ia data from Pantheon and the SH0ES estimate of the Hubble constant, and run an MCMC simulation to constrain the model parameters. We have found that all the models can significantly alleviate the H_0 tension, the best being the model **B**, for which an energy injection of $f_{\text{EDE}} = 0.082 \pm 0.029$ at the redshift $\log_{10} z_c = 3.510^{+0.044}_{-0.053}$ leads to an inferred value of the Hubble rate today of $H_0 = (70.9 \pm 1.1) \text{ km s}^{-1} \text{ Mpc}^{-1}$ at 68% CL.

As noticed in the literature, EDE models change the best-fit cosmological parameters from Λ CDM such as n_s , A_s and ω_c . This could lead to tension with large scale structure observations such as weak gravitational lensing [35], although the conclusion depends on the CMB data used in the analysis [36]. Another interesting conse-

quence is the spectral index n_s , which tends to be larger than the one obtained in Λ CDM, $n_s \sim 0.98$. This has an interesting implication for inflationary models. For example, some inflation models based on α -attractors predict a larger n_s if reheating occurs gravitationally [42, 43]. These α -attractor inflation models can be combined with early dark energy models as a two field model. It will be interesting to revisit inflation models in the light of new constraints on n_s [62–64].

ACKNOWLEDGMENTS

MB acknowledges the Marco Polo program of the Uni-

versity of Bologna for supporting a visit to the Institute of Cosmology and Gravitation at the University of Portsmouth, where this work started. FF acknowledges contribution from the contract ASI/INAF for the Euclid mission n.2018-23-HH.0 and by ASI Grant 2016-24-H.0. AEG and KK received funding from the European Research Council under the European Unions Horizon 2020 research and innovation programme (grant agreement No. 646702 “CosTesGrav”). KK is also supported by the UK STFC ST/S000550/1. WTE is supported by an STFC consolidated grant, under grant no. ST/P000703/1. Numerical computations for this research were done on the Sciama High Performance Compute cluster, which is supported by the ICG, SEPNet, and the University of Portsmouth.

-
- [1] L. Verde, T. Treu and A. G. Riess, *Nature Astronomy* **2019** doi:10.1038/s41550-019-0902-0 [arXiv:1907.10625 [astro-ph.CO]].
 - [2] N. Aghanim *et al.* [Planck Collaboration], arXiv:1807.06209 [astro-ph.CO].
 - [3] A. G. Riess, S. Casertano, W. Yuan, L. M. Macri and D. Scolnic, *Astrophys. J.* **876** (2019) no.1, 85 doi:10.3847/1538-4357/ab1422 [arXiv:1903.07603 [astro-ph.CO]].
 - [4] A. G. Riess *et al.*, *Astrophys. J.* **861** (2018) no.2, 126 doi:10.3847/1538-4357/aac82e [arXiv:1804.10655 [astro-ph.CO]].
 - [5] K. C. Wong *et al.*, arXiv:1907.04869 [astro-ph.CO].
 - [6] W. L. Freedman *et al.*, doi:10.3847/1538-4357/ab2f73 arXiv:1907.05922 [astro-ph.CO].
 - [7] W. Yuan, A. G. Riess, L. M. Macri, S. Casertano and D. Scolnic, *Astrophys. J.* **886** (2019) 61 doi:10.3847/1538-4357/ab4bc9 [arXiv:1908.00993 [astro-ph.GA]].
 - [8] W. L. Freedman *et al.*, doi:10.3847/1538-4357/ab7339 arXiv:2002.01550 [astro-ph.GA].
 - [9] L. Knox and M. Millea, *Phys. Rev. D* **101** (2020) no.4, 043533 doi:10.1103/PhysRevD.101.043533 [arXiv:1908.03663 [astro-ph.CO]].
 - [10] J. L. Bernal, L. Verde and A. G. Riess, *JCAP* **1610** (2016) 019 doi:10.1088/1475-7516/2016/10/019 [arXiv:1607.05617 [astro-ph.CO]].
 - [11] K. Aylor, M. Joy, L. Knox, M. Millea, S. Raghunathan and W. L. K. Wu, *Astrophys. J.* **874** (2019) no.1, 4 doi:10.3847/1538-4357/ab0898 [arXiv:1811.00537 [astro-ph.CO]].
 - [12] L. Lancaster, F. Y. Cyr-Racine, L. Knox and Z. Pan, *JCAP* **1707** (2017) 033 doi:10.1088/1475-7516/2017/07/033 [arXiv:1704.06657 [astro-ph.CO]].
 - [13] M. A. Buen-Abad, M. Schmaltz, J. Lesgourgues and T. Brinckmann, *JCAP* **1801** (2018) 008 doi:10.1088/1475-7516/2018/01/008 [arXiv:1708.09406 [astro-ph.CO]].
 - [14] F. D’Eramo, R. Z. Ferreira, A. Notari and J. L. Bernal, *JCAP* **1811** (2018) 014 doi:10.1088/1475-7516/2018/11/014 [arXiv:1808.07430 [hep-ph]].
 - [15] C. D. Kreisch, F. Y. Cyr-Racine and O. Dor, arXiv:1902.00534 [astro-ph.CO].
 - [16] N. Blinov, K. J. Kelly, G. Z. Krnjaic and S. D. McDermott, *Phys. Rev. Lett.* **123** (2019) no.19, 191102 doi:10.1103/PhysRevLett.123.191102 [arXiv:1905.02727 [astro-ph.CO]].
 - [17] C. Umilt, M. Ballardini, F. Finelli and D. Paoletti, *JCAP* **1508** (2015) 017 doi:10.1088/1475-7516/2015/08/017 [arXiv:1507.00718 [astro-ph.CO]].
 - [18] M. Ballardini, F. Finelli, C. Umilt and D. Paoletti, *JCAP* **1605** (2016) 067 doi:10.1088/1475-7516/2016/05/067 [arXiv:1601.03387 [astro-ph.CO]].
 - [19] M. X. Lin, M. Raveri and W. Hu, *Phys. Rev. D* **99** (2019) no.4, 043514 doi:10.1103/PhysRevD.99.043514 [arXiv:1810.02333 [astro-ph.CO]].
 - [20] M. Rossi, M. Ballardini, M. Braglia, F. Finelli, D. Paoletti, A. A. Starobinsky and C. Umilt, *Phys. Rev. D* **100** (2019) no.10, 103524 doi:10.1103/PhysRevD.100.103524 [arXiv:1906.10218 [astro-ph.CO]].
 - [21] J. Sol Peracaula, A. Gomez-Valent, J. de Cruz Prez and C. Moreno-Pulido, *Astrophys. J. Lett.* **886** (2019) no.1, L6 doi:10.3847/2041-8213/ab53e9 [arXiv:1909.02554 [astro-ph.CO]].
 - [22] M. Zumalacarregui, arXiv:2003.06396 [astro-ph.CO].
 - [23] G. Ballesteros, A. Notari and F. Rompineve, arXiv:2004.05049 [astro-ph.CO].
 - [24] M. Braglia, M. Ballardini, W. T. Emond, F. Finelli, A. E. Gumrukcuoglu, K. Koyama and D. Paoletti, arXiv:2004.11161 [astro-ph.CO].
 - [25] M. Ballardini, M. Braglia, F. Finelli, D. Paoletti, A. A. Starobinsky and C. Umilt, arXiv:2004.14349 [astro-ph.CO].
 - [26] V. Poulin, T. L. Smith, T. Karwal and M. Kamionkowski, *Phys. Rev. Lett.* **122** (2019) no.22, 221301 doi:10.1103/PhysRevLett.122.221301 [arXiv:1811.04083 [astro-ph.CO]].
 - [27] P. Agrawal, F. Y. Cyr-Racine, D. Pinner and L. Randall, arXiv:1904.01016 [astro-ph.CO].
 - [28] S. Alexander and E. McDonough, *Phys. Lett. B* **797** (2019) 134830 doi:10.1016/j.physletb.2019.134830 [arXiv:1904.08912 [astro-ph.CO]].
 - [29] M. X. Lin, G. Benevento, W. Hu and M. Raveri, *Phys. Rev. D* **100** (2019) no.6, 063542 doi:10.1103/PhysRevD.100.063542 [arXiv:1905.12618 [astro-ph.CO]].

- [30] T. L. Smith, V. Poulin and M. A. Amin, Phys. Rev. D **101** (2020) no.6, 063523 doi:10.1103/PhysRevD.101.063523 [arXiv:1908.06995 [astro-ph.CO]].
- [31] F. Niedermann and M. S. Sloth, arXiv:1910.10739 [astro-ph.CO].
- [32] K. V. Berghaus and T. Karwal, Phys. Rev. D **101** (2020) no.8, 083537 doi:10.1103/PhysRevD.101.083537 [arXiv:1911.06281 [astro-ph.CO]].
- [33] J. Sakstein and M. Trodden, Phys. Rev. Lett. **124** (2020) no.16, 161301 doi:10.1103/PhysRevLett.124.161301 [arXiv:1911.11760 [astro-ph.CO]].
- [34] N. Kaloper, Int. J. Mod. Phys. D **28** (2019) no.14, 1944017 doi:10.1142/S0218271819440176 [arXiv:1903.11676 [hep-th]].
- [35] J. C. Hill, E. McDonough, M. W. Toomey and S. Alexander, arXiv:2003.07355 [astro-ph.CO].
- [36] A. Chudaykin, D. Gorbunov and N. Nedelko, arXiv:2004.13046 [astro-ph.CO].
- [37] R. Kallosh and A. Linde, JCAP **1307** (2013) 002 doi:10.1088/1475-7516/2013/07/002 [arXiv:1306.5220 [hep-th]].
- [38] R. Kallosh, A. Linde and D. Roest, JHEP **1311** (2013) 198 doi:10.1007/JHEP11(2013)198 [arXiv:1311.0472 [hep-th]].
- [39] M. Galante, R. Kallosh, A. Linde and D. Roest, Phys. Rev. Lett. **114** (2015) no.14, 141302 doi:10.1103/PhysRevLett.114.141302 [arXiv:1412.3797 [hep-th]].
- [40] E. V. Linder, Phys. Rev. D **91** (2015) no.12, 123012 doi:10.1103/PhysRevD.91.123012 [arXiv:1505.00815 [astro-ph.CO]].
- [41] C. Garcia-Garcia, E. V. Linder, P. Ruz-Lapuente and M. Zumalacregui, JCAP **1808** (2018) 022 doi:10.1088/1475-7516/2018/08/022 [arXiv:1803.00661 [astro-ph.CO]].
- [42] K. Dimopoulos and C. Owen, JCAP **1706** (2017) 027 doi:10.1088/1475-7516/2017/06/027 [arXiv:1703.00305 [gr-qc]].
- [43] Y. Akrami, R. Kallosh, A. Linde and V. Vardanyan, JCAP **1806** (2018) 041 doi:10.1088/1475-7516/2018/06/041 [arXiv:1712.09693 [hep-th]].
- [44] D. J. E. Marsh, Phys. Rept. **643** (2016) 1 doi:10.1016/j.physrep.2016.06.005 [arXiv:1510.07633 [astro-ph.CO]].
- [45] V. Poulin, T. L. Smith, D. Grin, T. Karwal and M. Kamionkowski, Phys. Rev. D **98** (2018) no.8, 083525 doi:10.1103/PhysRevD.98.083525 [arXiv:1806.10608 [astro-ph.CO]].
- [46] B. Audren, J. Lesgourgues, K. Benabed and S. Prunet, JCAP **1302** (2013) 001 doi:10.1088/1475-7516/2013/02/001 [arXiv:1210.7183 [astro-ph.CO]].
- [47] T. Brinckmann and J. Lesgourgues, Phys. Dark Univ. **24** (2019) 100260 doi:10.1016/j.dark.2018.100260 [arXiv:1804.07261 [astro-ph.CO]].
- [48] J. Lesgourgues, arXiv:1104.2932 [astro-ph.IM].
- [49] D. Blas, J. Lesgourgues and T. Tram, JCAP **1107** (2011) 034 doi:10.1088/1475-7516/2011/07/034 [arXiv:1104.2933 [astro-ph.CO]].
- [50] N. Aghanim *et al.* [Planck Collaboration], arXiv:1907.12875 [astro-ph.CO].
- [51] Y. Akrami *et al.* [Planck Collaboration], arXiv:1807.06205 [astro-ph.CO].
- [52] S. Alam *et al.* [BOSS Collaboration], Mon. Not. Roy. Astron. Soc. **470** (2017) no.3, 2617 doi:10.1093/mnras/stx721 [arXiv:1607.03155 [astro-ph.CO]].
- [53] A. J. Ross *et al.* [BOSS Collaboration], Mon. Not. Roy. Astron. Soc. **464** (2017) no.1, 1168 doi:10.1093/mnras/stw2372 [arXiv:1607.03145 [astro-ph.CO]].
- [54] M. Vargas-Magaa *et al.*, Mon. Not. Roy. Astron. Soc. **477** (2018) no.1, 1153 doi:10.1093/mnras/sty571 [arXiv:1610.03506 [astro-ph.CO]].
- [55] F. Beutler *et al.* [BOSS Collaboration], Mon. Not. Roy. Astron. Soc. **464** (2017) no.3, 3409 doi:10.1093/mnras/stw2373 [arXiv:1607.03149 [astro-ph.CO]].
- [56] D. M. Scolnic *et al.*, Astrophys. J. **859** (2018) no.2, 101 doi:10.3847/1538-4357/aab9bb [arXiv:1710.00845 [astro-ph.CO]].
- [57] C. P. Ma and E. Bertschinger, Astrophys. J. **455** (1995) 7 doi:10.1086/176550 [astro-ph/9506072].
- [58] A. Lewis, arXiv:1910.13970 [astro-ph.IM].
- [59] N. Arkani-Hamed, L. Motl, A. Nicolis and C. Vafa, JHEP **0706** (2007) 060 doi:10.1088/1126-6708/2007/06/060 [hep-th/0601001].
- [60] S. Ferrara and R. Kallosh, Phys. Rev. D **94** (2016) no.12, 126015 doi:10.1103/PhysRevD.94.126015 [arXiv:1610.04163 [hep-th]].
- [61] R. Kallosh, A. Linde, T. Wrase and Y. Yamada, JHEP **1704** (2017) 144 doi:10.1007/JHEP04(2017)144 [arXiv:1704.04829 [hep-th]].
- [62] Y. Akrami *et al.* [Planck Collaboration], arXiv:1807.06211 [astro-ph.CO].
- [63] J. Martin, C. Ringeval and V. Vennin, Phys. Dark Univ. **5-6** (2014) 75 doi:10.1016/j.dark.2014.01.003 [arXiv:1303.3787 [astro-ph.CO]].
- [64] V. Vennin, K. Koyama and D. Wands, JCAP **1511** (2015) 008 doi:10.1088/1475-7516/2015/11/008 [arXiv:1507.07575 [astro-ph.CO]].

	Λ CDM	$p = 2, n = 0$ (A)	$p = 2, n = 4$ (B)	$p = 2, n = 4$ (C)
$10^2 \omega_b$	2.255 ± 0.014	2.274 ± 0.018	2.266 ± 0.018	2.283 ± 0.024
ω_c	0.11854 ± 0.00093	0.1265 ± 0.0036	0.1286 ± 0.0041	0.1250 ± 0.0038
$100 * \theta_s$	1.04205 ± 0.00028	1.04154 ± 0.00037	1.04134 ± 0.00039	1.04161 ± 0.00040
τ_{reio}	0.0603 ± 0.0076	$0.0602^{+0.0070}_{-0.0081}$	$0.0604^{+0.0068}_{-0.0082}$	$0.0583^{+0.0070}_{-0.0079}$
$\ln(10^{10} A_s)$	3.055 ± 0.015	3.067 ± 0.016	3.071 ± 0.016	3.064 ± 0.015
n_s	0.9701 ± 0.0037	0.9803 ± 0.0057	0.9795 ± 0.0054	0.9797 ± 0.0063
$\log_{10} z_c$	—	$3.550^{+0.074}_{-0.061}$	$3.510^{+0.044}_{-0.053}$	$3.528^{+0.058}_{-0.10}$
f_{EDE}	—	0.065 ± 0.026	0.082 ± 0.029	$0.048^{+0.029}_{-0.024}$
Θ_i	—	< 0.554	< 0.184	< 0.322
$\log_{10} \alpha$	—	$-0.3^{+1.4}_{-1.1}$	$0.65^{+1.5}_{-0.99}$	$0.0^{+1.6}_{-2.6}$
$\log_{10} V_0/\text{eV}^4$	—	$1.7^{+2.5}_{-1.7}$	$1.4^{+2.4}_{-1.7}$	$3.4^{+4.5}_{-4.0}$
$H_0 [\text{km s}^{-1} \text{Mpc}^{-1}]$	68.29 ± 0.42	70.28 ± 0.94	70.9 ± 1.1	69.88 ± 0.99
σ_8	0.8105 ± 0.0064	0.8255 ± 0.0090	0.8271 ± 0.0091	0.829 ± 0.012
$r_s [\text{Mpc}]$	147.21 ± 0.23	143.0 ± 1.8	142.0 ± 2.0	$143.7^{+2.5}_{-2.2}$
$\Delta\chi^2_{\text{min}}$		-9.68	-10.36	-8.66

TABLE I. Constraints on main and derived parameters considering Planck 2018 data (P18), BAO, Pantheon and SH0ES data. We report mean values and the 68% CL, except for the subset of EDE parameters $\{\Theta_i, \log_{10} V_0/\text{eV}^4, \log_{10} \alpha\}$ for which we report the 95% CL.